0026-895X/08/7403-872–883
MOLECULAR PHARMACOLOGY
U.S. Government work not protected by U.S. copyright
Mol Pharmacol 74:872–883, 2008

Vol. 74, No. 3
40808/3375561
Printed in U.S.A.

Combinatorial Antileukemic Disruption of Oxidative Homeostasis and Mitochondrial Stability by the Redox Reactive Thalidomide 2-(2,4-Difluoro-phenyl)-4,5,6,7-tetrafluoro-1*H*-isoindole-1,3(2*H*)-dione (CPS49) and Flavopiridol

Yun Ge, Jung S. Byun, Paola De Luca, Geraldine Gueron, Idalia M. Yabe, Sara G. Sadiq-Ali, William D. Figg, Jesse Quintero, Cynthia M. Haggerty, Quentin Q. Li, Adriana De Siervi, and Kevin Gardner

Laboratory of Receptor Biology and Gene Expression (Y.G., J.S.B., Q.Q.L., I.M.Y., S.G.S.-A., J.Q., C.M.H., A.D., K.G.) and Medical Oncology Branch (W.D.F.), National Cancer Institute, Bethesda, Maryland; and Department of Biochemistry, University of Buenos Aires, Argentina (A.D., P.D., G.G.)

Received August 9, 2007; accepted June 6, 2008

ABSTRACT

2-(2,4-Difluoro-phenyl)-4,5,6,7-tetrafluoro-1*H*-isoindole-1,3(2*H*)-dione (CPS49) is a member of a recently identified class of redox-reactive thalidomide analogs that show selective killing of leukemic cells by increasing intracellular reactive oxygen species (ROS) and targeting multiple transcriptional pathways. Flavopiridol is a semisynthetic flavonoid that inhibits cyclin-dependent kinases and also shows selective lethality against leukemic cells. The purpose of this study is to explore the efficacy and mechanism of action of the combinatorial use of the redox-reactive thalidomide CPS49 and the cyclin-dependent kinase inhibitor flavopiridol as a selective antileukemic therapeutic strategy. In combination, CPS49 and flavopiridol were found to induce selective cytotoxicity associated with mitochondrial dysfunction and elevations of ROS in leukemic cells ranging from additive to synergistic activity at low micromolar concentrations. Highest synergy was observed at the level of ROS generation with a strong correlation between cell-specific cytotoxicity and reciprocal coupling of drug-induced ROS elevation with glutathione depletion. Examination of the transcriptional targeting of CPS49 and flavopiridol combinations reveals that the drugs act in concert to initiate a cell specific transcriptional program that manipulates nuclear factor-κB (NF-κB), E2F-1, and p73 activity to promote enhanced mitochondrial instability by simultaneously elevating the expression of the proapoptotic factors *BAX*, *BAD*, *p73*, and *PUMA* while depressing expression of the antiapoptotic genes *MCL1*, *XIAP*, *BCL-xL*, *SURVIVIN*, and *MDM2.* The coadministration of CPS49 and flavopiridol acts through coordinate targeting of transcriptional pathways that enforce selective mitochondrial dysfunction and ROS elevation and is therefore a promising new therapeutic combination that warrants further preclinical exploration.

Cancer is a complex multigenic disease that results from the accumulation of a broad mixture of perturbations in cellular function that contributes to the maintenance and propagation of the malignant phenotype. Accordingly, most strategies for effective anticancer therapy employ combinatorial drug regimens designed to target one or more components within biological pathways that are thought to be critical for sustained tumor growth and survival. The long-term goal of these strategies is to provide therapeutic platforms that improve selective tumor killing while reducing undesired and off-target effects.

A well recognized feature of many transformed cells that distinguishes them from normal cells is their tendency to function at higher levels of oxidative stress (Litz et al., 2003; Pelicano et al., 2004; Trachootham et al., 2006). Although the

This work was funded through intramural research program of the National Cancer Institutes, National Institutes of Health.
Article, publication date, and citation information can be found at http://molpharm.aspetjournals.org.
doi:10.1124/mol.107.040808.

ABBREVIATIONS: ROS, reactive oxygen species; MMP, mitochondrial membrane permeability; Cdk, cyclin-dependent kinase; NF-κB, nuclear factor-κB; PBMC, peripheral-blood mononuclear cell; MTT, 3-[4,5-dimethylthiazol-2-yl]-2 5-diphenyl tetrazolium bromide; BSA-HBSS, bovine serum albumin in Hanks' buffered saline solution; MCF, mean channel fluorescence; PHA, phytohemagglutinin; PMA, phorbol 12-myristate 13-acetate; qRT-PCR, quantitative real-time polymerase chain reaction; CI, combination index; NAC, *N*-acetyl-cysteine; Rb, retinoblastoma protein.

precise mechanism that accounts for the elevated levels of reactive oxygen species (ROS) in tumor cells remains to be clarified, recent observation attributes this cellular state, in part, to mutations in components of the mitochondrial oxidative-phosphorylation chain combined with uncontrolled oncogenic signal transduction upstream of the mitochondria that cause them to be more prone to ROS leakage (Hlavatá et al., 2003; Pelicano et al., 2004). This observation has led to the development of therapeutic strategies to exploit this selective vulnerability of cancer cells by manipulating intracellular levels of ROS. The mitochondria therefore have become viewed as a high-impact biological target in strategies to exploit the redox vulnerabilities of malignant cells (Gottlieb and Thompson, 2003). Increased mitochondrial membrane permeability (MMP) plays a central role in determining cell fate through its ability to induce cell death by apoptosis or necrosis (Fiers et al., 1999; Newcomb, 2004; Zamzami et al., 2005). Key factors that regulate the levels of MMP include cellular redox status, calcium influx, and the targeting and function of Bcl-2 family members (Gottlieb et al., 2000; Zamzami et al., 2005). Pharmacological manipulation of these factors has therefore become a central aim in numerous therapeutic strategies.

Flavopiridol is a synthetically derived flavone that is known to target mitochondria and induce selective killing of leukemic cells through pathways linked to mitochondrial mediated apoptosis and necrosis (Sedlacek, 2001; Dai and Grant, 2003; Blagosklonny, 2004; Grant and Dent, 2004; Newcomb, 2004; Shapiro, 2006). Several recent studies have demonstrated its synergy with a variety of chemotherapeutic compounds (Grant and Roberts, 2003). Although flavopiridol has been defined as a cyclin-dependent kinase (Cdk) inhibitor, its effects have been shown to be widely pleiotropic against a variety of malignant cells (Dai and Grant, 2003; Blagosklonny, 2004; Grant and Dent, 2004; Newcomb, 2004; Shapiro, 2006). One major mechanism underlying its therapeutic effect involves its selective repression of transcriptional elongation (Chao and Price, 2001). Recent studies have shown that flavopiridol also has selective effects on gene expression by repressing nuclear factor-κB (NF-κB) transcriptional activation and preferentially influencing the levels of genes with short mRNA half-lives (Wittmann et al., 2003; Takada and Aggarwal, 2004). Because many of the BCL-2 family of proteins that promote mitochondrial stability have short half-lives and rely on NF-κB for induction, flavopiridol treatment can induce significant mitochondrial dysfunction resulting in increased MMP and both apoptotic and necrotic cell death (Lam et al., 2001; Wittmann et al., 2003).

We have described the identification and characterization of a novel functional class of thalidomide analogs referred to as redox-reactive thalidomides (Ge et al., 2006). These compounds inhibit NF-κB activity, increase intracellular calcium, and produce a rapid elevation of intracellular ROS that results in dissipation of the mitochondrial membrane potential and subsequent caspase-independent necrotic cell death (Ge et al., 2006). The shared targeting of both NF-κB activity and mitochondrial function by flavopiridol and the redox-reactive thalidomides suggested that the combinatorial use of these agents may produce more effective tumor cell killing. CPS49 is a redox-reactive thalidomide analog that has recently been shown to have effective cytotoxicity against lymphocytic leukemia cells, multiple myeloma, lung cancer, prostate cancer and endothelial cells (Ng et al., 2003, 2004; Kumar et al., 2005; Ge et al., 2006; Warfel et al., 2006). Like flavopiridol, it has been shown to have antiangiogenic potential (Ng et al., 2003; Newcomb, 2004).

In this study, we explore the potential therapeutic efficacy of the combined use of flavopiridol and CPS49 as an antileukemic strategy. We find that the compounds show varying degrees of synergistic, additive, and occasional antagonistic influences on leukemic cell killing based on their combined ability to repress NF-κB and destabilize mitochondrial function. Notably, we find that pretreatment of leukemic cells with low-dose, subcytotoxic levels of flavopiridol synergizes with CPS49 to cause selective leukemic cell death. A central mechanism underlying this combined synergy is the overlapping transcriptional targeting of tumor survival factors that regulate mitochondrial stability. Mitochondrial destabilizers, including Bax, Bak, and Bad, show enhanced up-regulation by flavopiridol and CPS49 combinations, whereas mitochondrial stabilizers, including BCL2, BCL-xL, and MCL1, are down-regulated. These findings suggest that the combined use of flavopiridol and redox-reactive thalidomides such as CPS49 should be evaluated as a feasible and practical antineoplastic regimen against leukemia and other malignancies.

Materials and Methods

Cell Lines and Cell Culture. Jurkat (acute lymphoblastic leukemia), HeLa (human epithelial-like cervical carcinoma), K562 (human chronic myelogenous leukemia), OPM2 (myeloma), HH (cutaneous T-cell lymphoma), LNCaP (prostate carcinoma), and RPMI-8226 (myeloma) cell lines were maintained in their respective growth media, as suggested by the American Type Culture Collection (Manassas, VA). Peripheral-blood mononuclear cells (PBMCs) were isolated by apheresis from healthy human blood donors. Cells were harvested after treatment with different concentrations of mitogens and/or drugs for various time points depending upon experimental design. The antioxidant *N*-acetyl-cysteine (NAC; 15 mM) was used to reverse the cytotoxic action of CPS49 and/or flavopiridol in Jurkat cells.

Cell Proliferation and Survival Assay. The viability and proliferation of cells were determined by MTT assay (Roche Applied Sciences, Indianapolis, IN) according to the manufacturer's instructions. The assay measures the dehydrogenase enzyme activity in metabolically active tumor cells, as reflected by the conversion of MTT to formazan, which is soluble in cell culture medium and was detected by absorbance at 570 nm. The production of formazan is proportional to the number of living cells, the intensity of the produced color serving as an indicator of the cell viability. In brief, the cells were plated at 1×10^5 cells/well in 96-well plates and cultured for 16 h. The MTT mixed with medium without serum was added to the cell cultures after removing the old medium. The plates were incubated at 37°C for 2 h, and the absorbance (A) at 570 nm was determined using a 96-well microplate reader (Molecular Devices, Sunnyvale, CA). The percentage cell survival was calculated using the background-corrected absorbance: % cell viability = $100 \times (1 -$ A of experimental well)/A of untreated control well. All assays were performed in triplicate in three independent experiments, and representative data are presented in Figs. 1 and 5. In flavopiridol pretreatment studies, flavopiridol was added to cells at a final concentration of 0.2 μM for 8 h.

Annexin Assay. Jurkat cells were exposed to increasing doses (0–10 μM) of flavopiridol and CPS49 either alone or in combination for 3 h as experimental designs. Jurkat cells were washed twice with ice-cold PBS and then resuspended in binding buffer at a concentration of 1×10^6 cells/ml. FITC-annexin V (5 μg; Invitrogen, Carlsbad, CA) were administered, and the cells were incubated in the dark for 20 min. FITC-annexin V was excited by primary laser at a band-

width of 488 nm and detected by FL-1 detector using FACScan (BD Biosciences, San Jose, CA). Ten thousand events were collected and data were analyzed by FlowJo (Tree Star Inc., Ashland, OR).

ROS Determinations. ROS generation was monitored by the increase in dichlorodihydrofluorescein diacetate fluorescence after drug stimulation. Cells were washed, resuspended in 1% bovine serum albumin in Hanks' buffered saline solution (BSA-HBSS) at 1×10^6 cells/ml, and maintained at 37°C for analysis. The oxidation-sensitive dye dichlorodihydrofluorescein diacetate (Invitrogen, Carlsbad, CA) was incubated with cells for 15 min at a final concentration of 2 μM. The incubation was ended by 3-fold dilution of the sample with ice-cold 1% BSA-HBSS. The cells were washed with ice-cold 1% BSA-HBSS before flow cytometric analysis. The stimulated increase in dye oxidation was calculated as the percentage increase in mean channel fluorescence (MCF) of drug-stimulated cells over that of unstimulated cells for each time point using the following equation: [(MCF (stimulated) − MCF (unstimulated)/MCF (unstimulated)] × 100. Results shown were an average of three independent experiments.

GSH Determinations. One million cells were lysed and incubated with 100 μM monochlorobimane at 37°C for 30 min. The formation of the fluorescent adduct was monitored in a final volume of 100 μl with a 1420 Victor2 Multilabel Counter (PerkinElmer Life and Analytical Sciences, Waltham, MA) with excitation at 385 nm and emission at 478 nm.

Measurement of Mitochondrial Membrane Potential. Changes in the mitochondrial membrane potential were measured by flow cytometry analysis of cells stained with 1,1′,3,3,3′,3′-hexamethylindodicarbocyanine iodide (Invitrogen), as recommended by the manufacturer. Flow cytometric analyses were performed with a FASCalibur flow cytometer using FlowJo. Data were collected for 10,000 events. All measurements were performed in duplicate and were representative of at least two independent experiments.

Antibodies and Immunoblot Analysis. The antibodies against Iκ-Bα, phospho-IκBα (Ser32), RelA (p65), phospho-Rb (ser807/811), and phospho-RelA (Ser536) were obtained from Cell Signaling Technology (Danvers, MA). Antibodies against phospho-pol II CTD (Ser2) were from Covance Research Products (Princeton, NJ), and the antibodies against β-actin, total Rb, and E2F-1 were purchased from Santa Cruz Biotechnology, Inc. (Santa Cruz, CA). Jurkat cells were preincubated for 15 min in the presence or absence of 10 μM CPS49 and/or flavopiridol before stimulation with phytohemagglutinin (PHA; 1 μg/ml) and phorbol 12-myristate 13-acetate (PMA; 50 ng/ml) for 15 min. Whole-cell lysates were prepared in a buffer containing 50 mM HEPES, 20 mM sodium pyrophosphate, 25 mM β-glycerophosphate, 50 mM sodium fluoride, 5 mM sodium molybdate, 5 mM EDTA, 150 mM orthophenanthrolene, 1% Nonidet P-40, 0.5% deoxycholate, 1% Triton X-100, 1% mammalian protease inhibitor (Sigma Chemicals, St. Louis, MO), and 0.2 mM Na_2VO_4. After protein quantitation using protein assay (Bio-Rad Laboratories, Hercules, CA), equal amounts (10–30 μg) of proteins were separated by SDS-polyacrylamide gel electrophoresis and blotted onto nitrocellulose membranes. The membrane was blocked with 5% nonfat dry milk in PBS, pH 7.5, containing 0.1% Tween 20 and incubated with a 1:1000 dilution of a primary antibody, as mentioned above, overnight at 4°C. The membrane was then washed with PBS containing 0.1% Tween 20 and incubated with a peroxidase-conjugated secondary antibody (1:1000; GE Healthcare, Chalfont St. Giles, Buckinghamshire, UK) for 1 h at room temperature. Specific antibody binding was detected using a chemiluminescence detection system (Amersham), according to the manufacturer's recommendations. After development, the membrane was stripped and reprobed with antibody against β-actin (1:1000) (Santa Cruz Biotechnology, Inc.) to confirm equal sample loading.

Analysis of mRNA Expression of Genes by Real-Time Reverse Transcription-Polymerase Chain Reaction (RT-PCR). Total cellular RNA was isolated from Jurkat cells using RNeasy Mini Kit (QIAGEN, Valencia, CA) and quantitated with a NanoDrop ND-1000 Spectrophotometer (NanoDrop Technologies, Wilmington, DE). RNA (1 μg) was reversely transcribed using QIAGEN Omniscript RT Kit as recommended by the manufacturer. Primer sequences were synthesized by Operon Biotechnologies, Inc. (Huntsville, AL). The primer sequences of the genes used in this study are shown in Table 1.

Quantitative real-time polymerase chain reaction (qRT-PCR) was performed with an ABI Prism 7000 Sequence Detection System (Applied Biosystems, Foster City, CA). The amplification of the genes was done in the following amplification conditions: each 25-μl reaction mixture contained 0.3 μM primers (both forward and reverse primers), 2 μl of template cDNA from reverse transcription, and 12.5 μl of 2× SYBR GreenER qPCR SuperMix (Invitrogen). Each reaction mixture was incubated at 50°C for 2 min and 95°C for 10-min hold, and then 50 cycles were performed for amplification at 95°C for 15 s and 60°C for 1 min. A melting-curve analysis that read every 0.3°C from 65° to 95°C was followed to assess the homogeneity of a PCR-amplified product. The results of qRT-PCR were analyzed using software provided by the manufacturer. The relative quantity of a specific mRNA was calculated with the comparative ΔC_t method on the basis of β-actin versus the gene of interest.

Statistical Analysis of Data. The significance of difference between experimental conditions was determined using the Student's *t* test for unpaired observations. A value of $P < 0.05$ was considered statistically significant. To assess the interactions between agents, median dose analysis was employed (CalcuSyn; Biosoft, Ferguson, MO) to calculate the combination index (CI) using experimental readout as the endpoint. Median dose analysis for CI was designed based on the multiple drug-effect equation derived from enzyme kinetic models as follows: $CI = (D)_1/(Dx)_1 + (D)_2/(Dx)_2 + (D)_1(D)_2/(Dx)_1(Dx)_2$, where $(D)_1$ and $(D)_2$ (in the numerators) indicate the doses of drug 1 and drug 2 in combination to obtain *x*% effects in the actual experiment, and $(Dx)_1$ and $(Dx)_2$ (in the denominators) indicate the doses of drug 1 and drug 2 alone to achieve *x*% effects (Chou and Talalay, 1984). CalcuSyn software was used to display the results of this analysis in the form of isobolograms, which are two-dimensional graphs that illustrates the interaction between two agents in terms of their antagonistic, additive, or synergistic effect on single biological measurement (e.g., cytotoxicity) (Loewe, 1953).

TABLE 1
Primer sequences

Gene Name	Accession Number	Sequence
β-Actin	NM_001101.2	5′-GCACAGAGCCTCGCCTT-3′ 5′-GTTGTCGACGACGAGCG-3′
Bad	NM_032989.1	5′-GGTAGGAGCTGTGGCGACT-3′ 5′-CAGGCCTCCTGTGGGAC-3′
Bax	NM_004324.3	5′-AGCTTCTTGGTGGACGCAT-3′ 5′-CAGAGGCGGGGTTTCATC-3′
Bcl-2	NM_000633.2	5′-GAGAAATCAAACAGAGGCCG-3′ 5′-CTGAGTACCTGAACCGGCA-3′
Bcl-X_L	NM_001191.2	5′-CTGCTGCATTGTTCCCATAG-3′ 5′-TTCAGTGACCTGACATCCCA-3′
Survivin	NM_001012271.1	5′-CTTTCTCCGCAGTTTCCTCA-3′ 5′-TTGGTGAATTTTTGAAACTGGA-3′
MDM2	NM_002392.2	5′-CCTGATCCAACCAATCACCT-3′ 5′-TGTTGTGAAAGAAGCAGTAGCA-3′
PUMA	NM_014417.2	5′-GTAAGGGCAGGAGTCCCAT-3′ 5′-GACGACCTCAACGCACAGTA-3′
XIAP	NM_001167.2	5′-TGATGTCTGCAGGTACACAAGTT-3′ 5′-GGACCCTCCCCTTGGAC-3′
MCL-1	NM_182763.1	5′-CATTCCTGATGCCACCTTCT-3′ 5′-TCGTAAGGACAAAACGGGAC-3′
p73	NM_005427.1	5′-CCCCATCAGGGGAGGTG-3′ 5′-AGGGGACGCAGCGAAAC-3′.

Results

The Combinatorial Addition of CPS49 and Flavopiridol Shows Selective Antileukemic Synergy That Improves with Low-Dose Flavopiridol Pretreatment. Jurkat, K562, HeLa, RPMI-8226, and donor PBMCs were each treated for 16 h with increasing concentrations of CPS49 (0–10 μM) and flavopiridol as single-drug treatments or in 1:1 combination (Fig. 1A). As shown by the viability curves in Fig. 1A, flavopiridol and CPS49 both show selective cytotoxicity against Jurkat cells. However, their cytotoxicity profiles are not identical because flavopiridol shows greater cytotoxicity against the multiple myeloma cell line 8226 than CPS49, as has been shown previously (Kumar et al., 2005), and requires levels of at least 20-fold to achieve an effect comparable with that of flavopiridol.

Although effective as single agents against Jurkat, the coadministration of both CPS49 and flavopiridol showed only mild additive to synergistic effects, with slight antagonism at high concentrations that can be objectively assessed by plotting the CI against the fraction affected (see *Materials and Methods*). This analysis yields an isobologram in which CI <1.0 indicates synergy, CI >1.0 indicates antagonism, and CI = 1.0 indicates additive influence of the drug combination (Fig. 1B and Table 2). These findings suggest that there may be a significant overlap between the pathways targeted by CPS49 and flavopiridol. However, the appearance of greater synergy at lower concentrations suggests that sequential pretreatment or "induction" of the cells with lower subcytotoxic concentrations of one of the drugs might improve their cytotoxicity against leukemic cells. Similar sequential strategies with low-dose flavopiridol have been shown to be effective in combination with the BCL-2 inhibitor HA14-1 (Pei et al., 2004). We therefore assessed the possible use of low-dose flavopiridol as an inducing agent before sequential combined

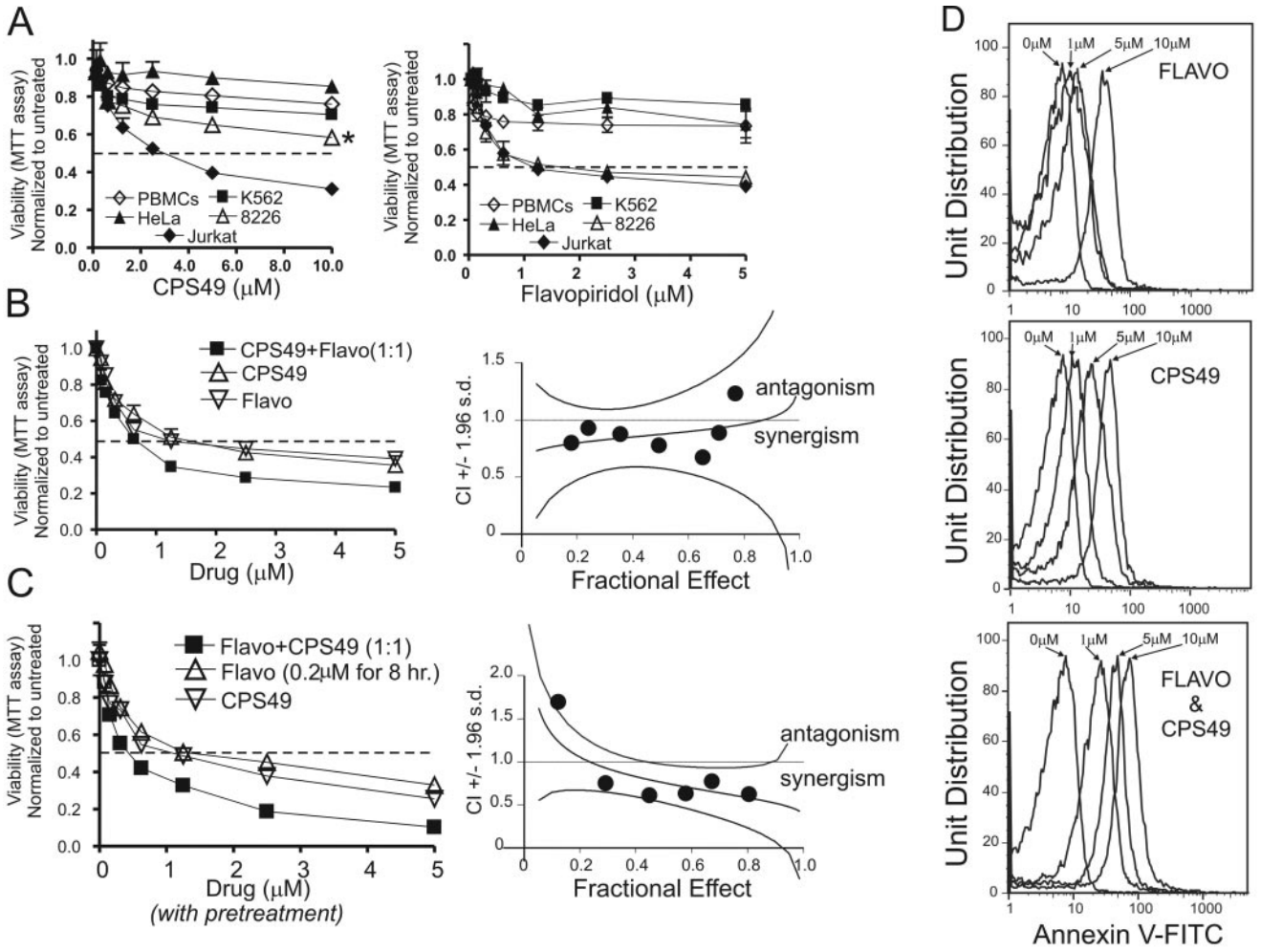

Fig. 1. Combinatorial treatment with CPS49 and flavopiridol shows selective cytotoxic synergy against transformed leukemic cells. A, PBMCs, Jurkat, K562, HeLa, and 8226 cells were incubated with increasing concentrations of CPS49 alone (left) or flavopiridol alone (right). Cell viability was measured by MTT assay at 16 h after the drug treatments. $*$, 20-fold higher concentrations of CPS49 were used in 8226 cells (left). B, Jurkat cells (left) were incubated with increasing concentrations (0–5 μM) of CPS49 alone, flavopiridol alone or CPS49 plus flavopiridol with a fixed ratio of 1:1. Cell viability was determined after 16-h incubation with the drugs. CI values (right) for each fractional effect were calculated using a commercially available software (Calcusyn; Biosoft). C, after 8-h pretreatment with 0.2 μM flavopiridol, Jurkat cells (left) were incubated with increasing concentrations (0–5 μM) of CPS49 alone, flavopiridol alone, or CPS49 plus flavopiridol (a fixed ratio of 1:1) for an additional 16 h, and cell viability was assessed at the termination of incubation. The viability of the Jurkat cells after 16-h exposure to flavopiridol at 0.2 μM was approximately 90%. The data presented are the means of three independent determinations after normalization to those of the untreated cells. CI values (right panel) for each fractional effect were calculated using the software, and a CI value <1.0 indicates synergism, CI = 1.0 indicates an additive effect, and CI > 1.0 indicates antagonism. D, fluorescence-activated cell sorting measurement of acute increase in annexin-positive staining of Jurkat cells 3 h after addition of increasing doses (0–10 μM) of flavopiridol and CPS49 either alone or in combination as indicated.

addition of flavopiridol and CPS49 (Fig. 1C). As shown in Fig. 1C and Table 2, 8-h pretreatment with 0.2 μM flavopiridol causes much more effective leukemic cell killing at higher drug concentrations and produces a more synergistic trend in the isobolograms (Fig. 1, B and C, right). Although this strategy produces more effective cell killing after prolonged incubation, it should be noted that more acute influences of cooperative targeting by combined treatment with CPS49 and flavopiridol treatment are readily detectable by annexin staining as early as 3 h after incubation in the absence of pretreatment (Fig. 1D).

CPS49 and Flavopiridol Combinations Produce Selective and Synergistic Depletion of GSH with Concomitant Elevation of Intracellular ROS. Both CPS49 and flavopiridol have been shown to alter the redox status of leukemic cells (Decker et al., 2001; Ge et al., 2006). To assess the selective combined influence of CPS49 and flavopiridol on the redox properties of primary and transformed cells the intracellular levels of ROS and GSH were assessed in cells treated with different combinations of flavopiridol and CPS49 after 1- and 16-h incubations, respectively (Fig. 2). When added as single agents, both flavopiridol and CPS49 produced significant elevation of ROS coupled with depletion of GSH in Jurkat cells (Fig. 2A). These effects were strikingly different from those of other cell types, including PBMCs, K562, HeLa, and 8226 cells, which show very little depletion of GSH and much smaller elevation in intracellular ROS (Fig. 2B). Quantitative analysis of the combined effects of flavopiridol and CPS49 on Jurkat show significant synergy for GSH depletion and ROS elevation (Table 2).

Synergistic Targeting of NF-κB Activation and the Mitochondrial Membrane Potential by Combinatorial Administration of Flavopiridol and CPS49. The mitochondria play a central role in regulating cellular redox status (Gottlieb and Thompson, 2003; Galluzzi et al., 2006). Both flavopiridol and redox-reactive thalidomides have been shown to reduce the mitochondrial membrane potential. To test their combined activity, the mitochondrial membrane potential in Jurkat cells was measured 1 and 3 h after single or combined treatment with increasing concentrations of flavopiridol and CPS49. When added as single agents, each compound produced reduction in mitochondrial membrane potential; however, their action together showed antagonism at higher concentrations, with moderate synergy at lower drug concentrations and shorter incubation intervals (Fig. 3A and Table 2).

NF-κB activation is a central component of a major transcriptional program that controls mitochondrial stability in mammalian cells (Lin and Karin, 2003; Luo et al., 2005). This is particularly the case for lymphoid cells. Numerous transcriptional targets of NF-κB are genes that control cellular survival, either at the level of maintaining mitochondrial stability (e.g., the BCL2 family of proteins) or by repressing cell-death inducing caspase activation (e.g., the inhibitor of apoptosis family of proteins). To test the combined influence of flavopiridol and CPS49 on NF-κB activation, Jurkat cells were stimulated 15 min with the mitogens PHA and PMA after brief preincubation with CPS49, flavopiridol, or the two combined. Whole-cell lysates were prepared and analyzed by immunoblot analysis for NF-κB activation (Fig. 3, B and C). As shown in Fig. 3B, PHA/PMA induces a robust phosphorylation of the inhibitor of $\kappa B\alpha$. This phosphorylation is significantly reduced after treatment with either CPS49 or flavopiridol and their combination nearly completely obliterates I-$\kappa B\alpha$ phosphorylation (Fig. 3B). Likewise, PHA/PMA produces an equally robust increase in phosphorylation of the RelA (p65) NF-κB subunit that is synergistically squelched by flavopiridol and CPS49 (Fig. 3C).

Prior studies have shown that flavopiridol induces stabilization of E2F-1 (Jiang et al., 2003). The up-regulated transcriptional targets of E2F-1 include *p73*, which leads to increased expression of the mitochondrial destabilizers *BAX*, *BAD*, and *PUMA* (Irwin et al., 2000; Hitchens and Robbins, 2003). The down-regulated targets of E2F-1 included *MCL1*, a *BCL2* family member that stabilizes mitochondria in lymphoid cells (Craig, 2002; Rosato et al., 2007). It is noteworthy that although treatment of Jurkat cells with flavopiridol stabilizes E2F-1 protein levels, CPS49 does not (Fig. 3D). In fact, the combination of flavopiridol and CPS49 seems to slightly antagonize E2F1 levels in both resting and stimulated Jurkat cells.

A common mode of flavopiridol action is through induction of caspase activation (for review, see Newcomb, 2004). This activity is notably distinct from redox-reactive thalidomides, which act through caspase independent pathways (Ge et al., 2006). To determine whether there is any influence of CPS49 on flavopiridol-induced caspase activation, Jurkat cells were treated with each agent alone or in combination and then analyzed for the activation of caspase 3 cleavage by Western blot. As shown in Fig. 3E, flavopiridol clearly activates caspase 3 cleavage whereas CPS49 does not. Combined addition of CPS49 with flavopiridol also fails to increase the

TABLE 2
Differential synergism between CPS49 and flavopiridol: cytotoxicity, mitochondrial membrane potential, and ROS

Cytotoxicity (MTT)								Mitochondrial Membrane Potential[a] with Pretreatment				ROS with Pretreatment			
No Pretreatment				With Pretreatment											
CPS49	Flavo	Fa	CI	CPS49	Flavo	Fa	CI	CPS49	Flavo	Fa	CI	CPS49	Flavo	Fa	CI
μM				μM	μM			μM	μM			μM	μM		
0.078125	0.078125	0.176	0.817	0.078125	0.078125	0.118	1.707	1	1	0.264	0.5	1	1	0.136	0.876
0.15625	0.15625	0.245	0.924	0.15625	0.15625	0.295	0.75	5	5	0.401	0.926	2	2	0.221	1.044
0.3125	0.3125	0.358	0.874	0.3125	0.3125	0.447	0.635	10	10	0.480	1.12	5	5	0.377	1.333
0.625	0.625	0.500	0.787	0.625	0.625	0.581	0.64					10	10	1.000	1.81×10^{-8}
1.25	1.25	0.653	0.661	1.25	1.25	0.673	0.775								
2.5	2.5	0.714	0.9	2.5	2.5	0.814	0.612								
5	5	0.767	1.232	5	5	0.897	0.531								

Fa, fraction affected by the dose; CI, combination index that defines additive (CI = 1.0), synergistic (CI < 1.0), or antagonistic (CI > 1.0) effects.
[a] Measured at 3 h. All measurements were conducted with Jurkat leukemic T cells.

caspase cleavage beyond that elicited by flavopiridol treatment alone.

Combinatorial Treatment with CPS49 and Flavopiridol Coordinates a Transcriptional Program That Triggers Destabilization of Mitochondrial Function. The coordinated targeting of NF-κB and E2F-1 pathways by the coadministration of flavopiridol and CPS49 implies that this regimen should have demonstrable effects on genes that control cell death and survival. To investigate this question, we examined the influence of combinations of flavopiridol and CPS49 on proapoptotic and antiapoptotic gene sets (Fig. 4). The set of proapoptotic genes includes *BAX*, *BAD*, *p73*, and *PUMA* (Fig. 4A). Flavopiridol shows up-regulation of all four genes, whereas CPS49 showed up-regulation of all but *PUMA* in both resting and PHA/PMA stimulated cells (Fig. 4A). It is noteworthy that the coaddition of CPS49 and flavopiridol showed no additional increase in expression of the proapoptotic genes and, in fact, showed mild antagonism for p73 expression.

Both flavopiridol and CPS49 show significant repression of the six antiapoptotic genes we tested, including *MCL1*, *XIAP*, *BCL-xL*, *BCL2*, *survivin*, and *MDM2* (Fig. 4B). For each of these genes, CPS49 produced more significant repression than flavopiridol in both resting and PHA/PMA stimulated cells. Again, the combination of CPS49 and flavopiridol did not synergize to induce repression and, in some instances, the pairing was antagonistic.

Cytotoxicity and Transcriptional Targeting of p73 and PUMA by CPS49 and Flavopiridol Is Partially Inhibited by Free Radical Scavengers. Because both flavopiridol and CPS49 produce elevations in ROS, we analyzed the influence of the free radical scavenger, NAC, on the cytotoxicity profile of CPS49, flavopiridol, and the two combined. As shown in Fig. 4C, NAC partially rescued cellular viability when added under all three conditions. Cytotoxicity of flavopiridol added as a single agent seemed to be the most sensitive to NAC (Fig. 4C). To determine whether the ROS generated by these compounds plays any role in the mechanism of transcriptional activation of downstream proapoptotic targets, we tested whether or not NAC could repress the ability of CPS49 and/or flavopiridol to elevate p73 and PUMA transcription (Fig. 4D). As shown in Fig. 4D, although NAC was partially effective at reducing the cytotoxicity of both

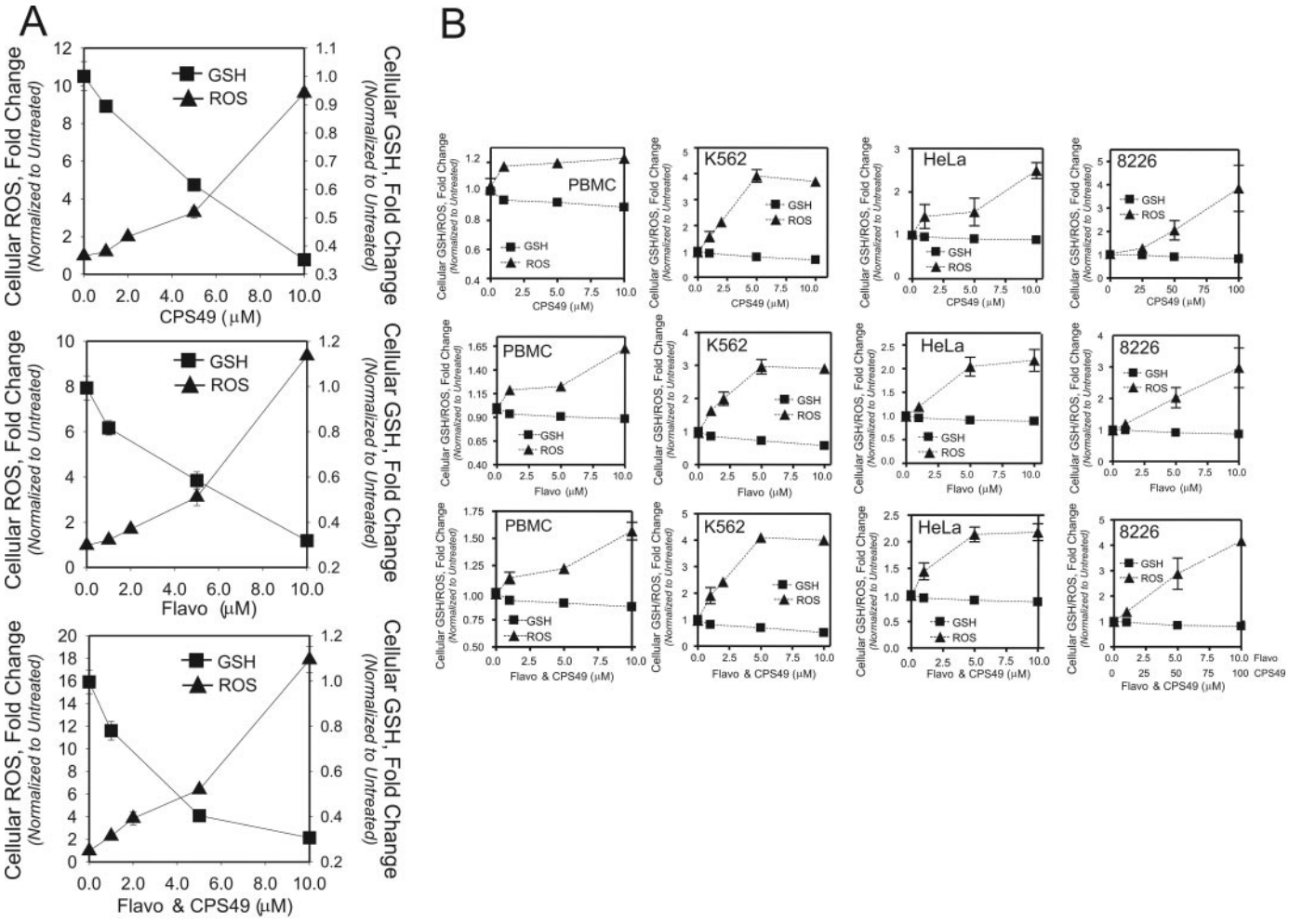

Fig. 2. CPS49 and flavopiridol demonstrate selective disruption of homeostasis of intracellular GSH and ROS in transformed leukemia cells. A, the profile of ROS generation in Jurkat cells after 1-h drug treatment and the profile of cellular GSH depletion in Jurkat cells after 16-h exposure to CPS49 alone (top), flavopiridol alone (middle), or CPS49 plus flavopiridol (bottom) at the indicated concentrations. B, the profile of ROS generation in PBMCs, K562, HeLa, and 8226 cells after 1-h drug treatment and the profile of intracellular GSH depletion in these cells after 16-h drug exposure to CPS49 alone (top), flavopiridol alone (middle), or CPS49 plus flavopiridol (bottom) at the concentrations indicated. GSH and ROS were measured as described under *Materials and Methods*. The data shown are the means of three independent experiments after being normalized to those of the untreated cells.

flavopiridol and/or CPS49 combinations in Jurkat, influences on the transcriptional targets seemed to be more potent.

Combinatorial Synergy and Transcriptional Targeting by CPS49 and Flavopiridol after Low-Dose Flavopiridol Pretreatment Is Highly Cell-Type Specific. Our data have shown thus far that combination therapy with CPS49 and flavopiridol shows significant synergy that can be enhanced by low-dose flavopiridol pretreatment. To test the cell-type specificity of this treatment regimen, five additional cell lines, including HeLa (cervical carcinoma), LNCaP (prostate carcinoma), HH (cutaneous T-cell lymphoma), OPM2 (myeloma), and 8226 (myeloma) were exposed to increasing doses of flavopiridol, CPS49, and CPS49/flavopiridol combined each after 8-h pretreatment with 0.2 μM flavopiridol (Fig. 5A). As shown in Fig. 5A, CPS49/flavopiridol treatment showed significant cytotoxicity against the HH, OPM2, and 8226 cell lines but minimal effect on HeLa and LNCaP cells. Moreover, quantitative assessment of the synergy between CPS49 and flavopiridol showed significant synergy against both myeloma cell lines OPM2 and 8226 with additive to antagonistic influence on HH cells (Fig. 5B and Table 3). It is interesting to note that in terms of cytotoxicity, pretreatment with flavopiridol dramatically increased the potency of CPS49 against both myeloma cell lines (Fig. 5A). This is also reflected in the higher levels of synergy between CPS49 and flavopiridol, after low-dose pretreatment compared with Jurkat even though this combination is still significantly more cytotoxic against Jurkat (compare Figs. 1B and 5A and Tables 2 and 3).

The addition of combinations of CPS49 and flavopiridol added in the absence of pretreatment as in Fig. 4 showed overlapping but distinct transcriptional targeting of the myeloma cell line 8226. CPS49, flavopiridol, and the two combined did not produce significant up-regulation of proapoptotic genes. Instead, most of these genes were repressed by flavopiridol, CPS49 alone had little effect, and the combination had little influence over flavopiridol added alone (Fig. 6A). Similar to Jurkat, flavopiridol produced significant inhibition of pro-survival genes that stabilize mitochondrial integrity (Fig. 6B). However, consistent with prior studies indicating that higher levels of CPS49 were necessary to influence 8226 growth and viability (Kumar et al., 2005; Ge et al., 2006), CPS49 was not effective at influencing pro-survival gene expression at the maximum concentrations used in this study (10 μM). Finally, pretreatment of Jurkat cells with low levels (0.2 μM) of flavopiridol show selective repression of CDK9 activity, as demonstrated by the preferential decrease in pol II serine 2 phosphorylation as opposed to substrates targeted during cell cycle progression, such as serine 807/811 on Rb (Fig. 6C).

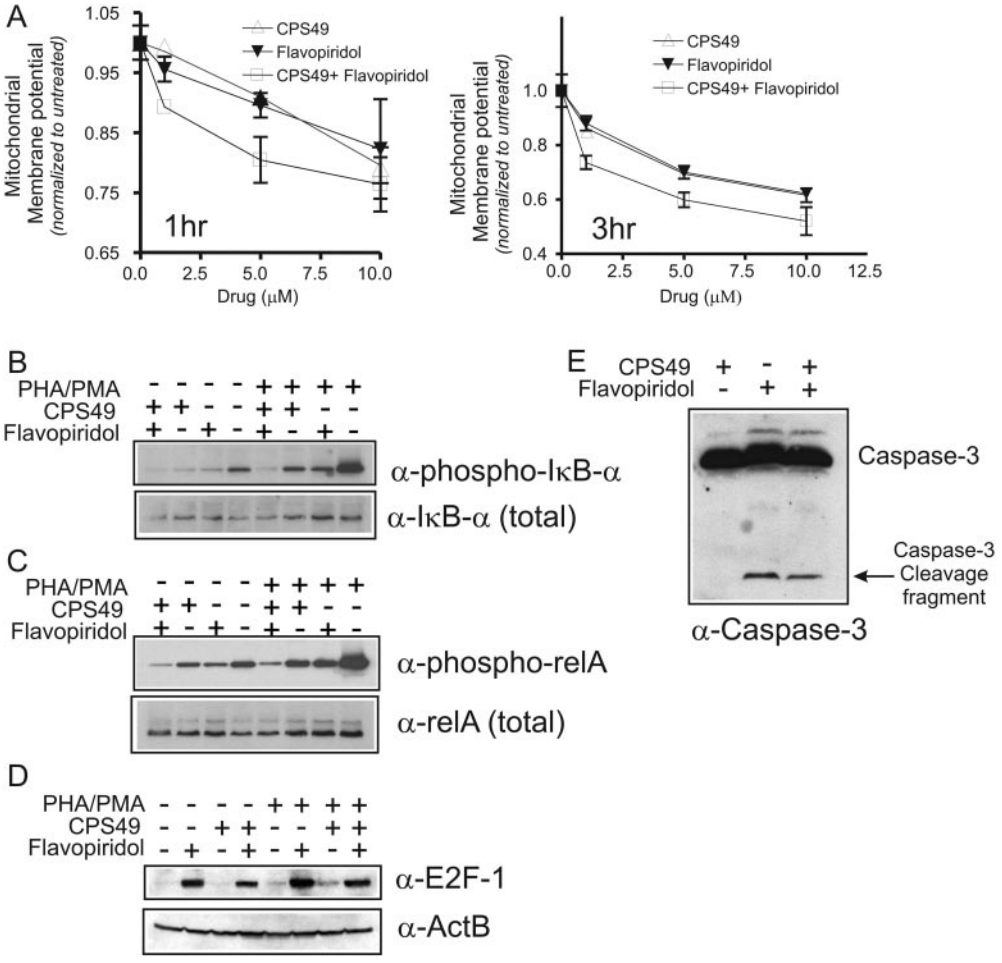

Fig. 3. CPS49 and flavopiridol combinations synergistically reduce the mitochondrial membrane potential and NF-κB activation but differentially influence E2F-1 and caspase activation in transformed leukemic cells. A, flow cytometric measurement of CPS49- and/or flavopiridol-mediated loss of mitochondrial membrane potential in Jurkat cells after exposure to CPS49, flavopiridol, and CPS49 plus flavopiridol, respectively, for 1 h (left) or 3 h (right), as outlined above. B, Jurkat cells were preincubated for 15 min in the presence or absence of 10 μM CPS49 and/or flavopiridol before stimulation with PHA (1 μg/ml) and PMA (50 ng/ml) for an additional 15 min. Whole cellular lysates were then prepared for immunoblot analysis of phospho-IκB-α (Ser32) and IκB-α (total) levels in the whole-cell lysates from the Jurkat cells as described under *Materials and Methods*. C, immunoblot analysis of phospho-relA (Ser536) and relA (p65) levels in the whole-cell lysates from the Jurkat cells treated with the drugs as outlined above. D, immunoblot analysis of E2F-1 and β-actin (ActB) protein levels. E, immunoblot analysis of caspase 3 in whole-cell lysates from Jurkat cells pretreated 8 h with 0.2 μM flavopiridol followed by the addition of 10 μM CPS49 and flavopiridol alone or in combination for an additional 8 h.

Discussion

Despite its successful performance in numerous preclinical studies, the advance of flavopiridol to clinical trials has been disappointing. When used as a single agent, flavopiridol produced the stabilization of disease expected as a result of its cytostatic activity as a general Cdk inhibitor. However, few studies showed any additional response (Senderowicz et al., 1998; Tan et al., 2002; Blagosklonny, 2004; Shapiro, 2004). The mechanism through which flavopiridol is able to induce apoptosis through inappropriate stabilization E2F-1 activity in S-phase formed the rationale for its combined use with compounds that forced S-phase accumulation, such as traditional DNA-damaging agents and mitotic poisons. However, several clinical trials employing such combination with flavopiridol have yet to yield convincing results. Challenges that have emerged from these studies involve defining the optimum sequence, dose, and timing of drug administration and identifying practical biomarkers for therapeutic end points.

This is the first study of the efficacy of the combinatorial use of a cyclin-dependent kinase inhibitor and a thalidomide-derived compound. Our rationale for the combined use of the redox-reactive thalidomides with flavopiridol is distinct and independent of its effect on cell cycle. Instead, our hypothesis is formulated based on the ability of flavopiridol and CPS49 to target mitochondrial stability at multiple nodes in multiple pathways that lead to cell death. Because the reciprocal targeting of both proapoptotic and prosurvival pathways is reinforced by the combined action of CPS49 and flavopiridol, we feel that this combination merits further preclinical development (Fig. 6D).

Our approach of combining sequential low-dose flavopiridol pretreatment with higher dose flavopiridol and CPS49 is counter to many approaches that have been advocated thus far for combination therapy using flavopiridol (Blagosklonny, 2004; Shapiro, 2004). Again, this is based on the more selective transcriptional targeting of short-lived transcripts for pro-survival genes at (0.2 μM) flavopiridol, which has been reported as the achievable plasma concentration of low-dose flavopiridol treatment in clinical trials (Senderowicz et al., 1998). We feel that during this "induction phase," the resulting decrease in *BCL2*, *BCL-xL*, and *MCL1* increases the vulnerability of the mitochondria of malignant cells to further insult by the short-term administration of higher doses of flavopiridol combined with CPS49. Surprisingly, this approach also showed a dramatic increase in cytotoxicity of CPS49 against myeloma cells. This is apparent when comparing Figs. 1A and 5B, where 8-h preincubation with 0.2 μM

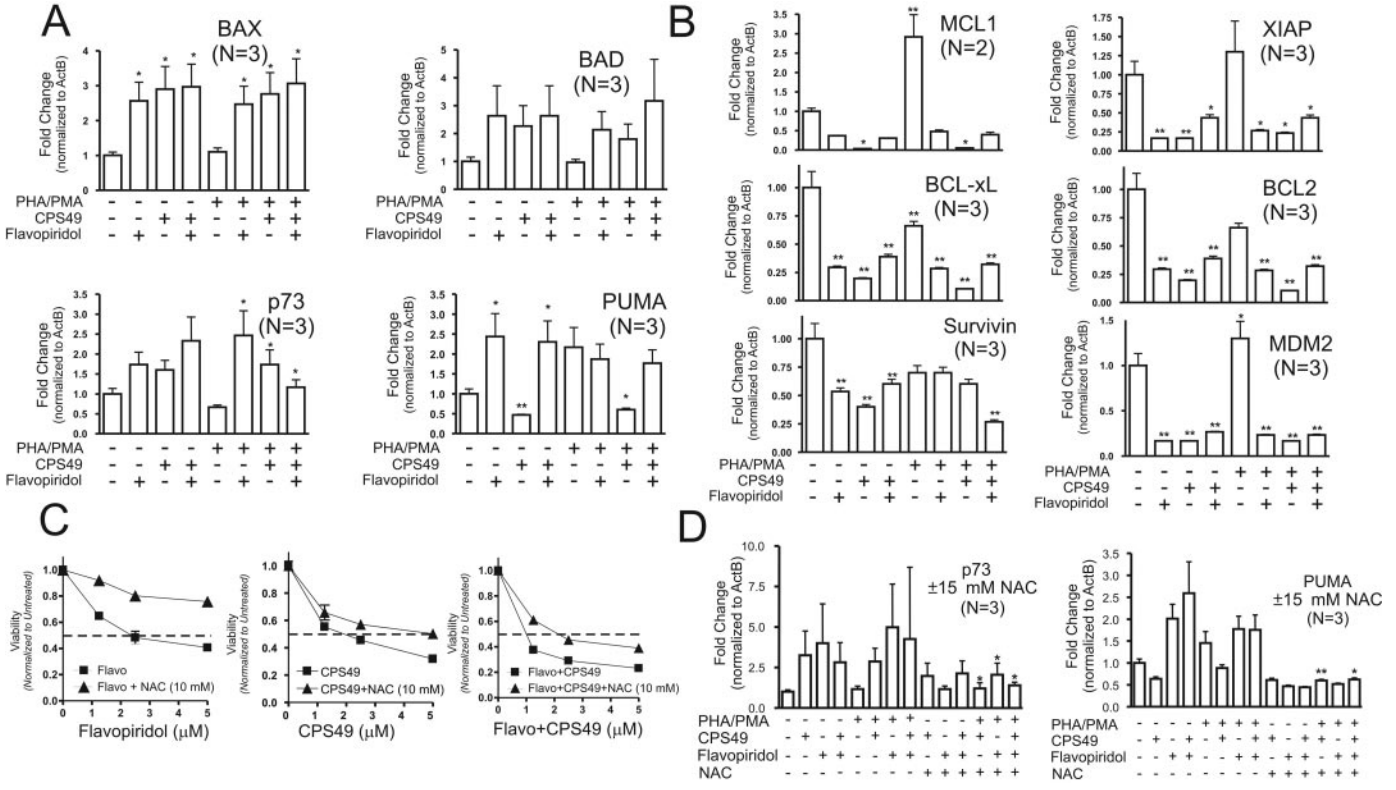

Fig. 4. CPS49 and flavopiridol preferentially up-regulate the expression of proapoptotic genes, but simultaneously down-regulate the expression of antiapoptotic genes. A, Jurkat cells were stimulated with 1 μg/ml PHA and 50 ng/ml PMA in the presence or absence of 10 μM CPS49 and/or flavopiridol for 3 h. Total cellular RNA was then isolated from the cell lysates and cDNA was synthesized. mRNA levels of *BAX*, *BAD*, *p73*, and *PUMA* gene expression were analyzed by qRT-PCR, as described under *Materials and Methods*. B, mRNA levels of *MCL1*, *XIAP*, *BCL-2*, *BCL-XL*, *Survivin*, and *MDM2* gene expression were assessed by qRT-PCR analysis in the Jurkat cells treated with the drugs, as outlined above. The data presented are the means of three separate determinations after being normalized to those of the housekeeping gene β-actin. *, $P < 0.05$ and **, $P < 0.01$ versus the untreated controls. C, the reversal of CPS49- and/or flavopiridol-induced cell killing by 10 mM NAC, an antioxidant, in Jurkat cells, as determined by MTT assay. The data shown are the means of three separate experiments after being normalized to those of the untreated cells. D, Jurkat cells were stimulated for 3 h with PHA (1 μg/ml) and PMA (50 ng/ml) in the presence or absence of 10 μM CPS49 and/or flavopiridol, as well as 15 mM NAC. Total cellular RNA was then isolated from the cell lysates and cDNA was synthesized. The reversal of CPS49- and flavopiridol-mediated mRNA expression of p73 (left) and PUMA (right) genes by NAC was assessed by qRT-PCR analysis, as described under *Materials and Methods*. *, $P < 0.05$; **, $P < 0.01$ for the cells with NAC treatment versus the cells without NAC treatment.

flavopiridol increased the cytotoxicity of CPS49 nearly 20-fold and was further effective with subsequent coadministration with micromolar concentrations of flavopiridol in combination with CPS49. Although the level of cell killing in myeloma is much lower than in Jurkat, this finding indicates that further investigation of the potential of flavopiridol to increase the efficacy of fluoride-substituted thalidomide compounds against myeloma is justified. Future studies will be needed to sort out the precise mechanisms that differentiate the CPS49 sensitivity of myeloma cells and Jurkat cells, although the increased impairment of mitochondrial stability and possibly antioxidant reserve by flavopiridol pretreat-

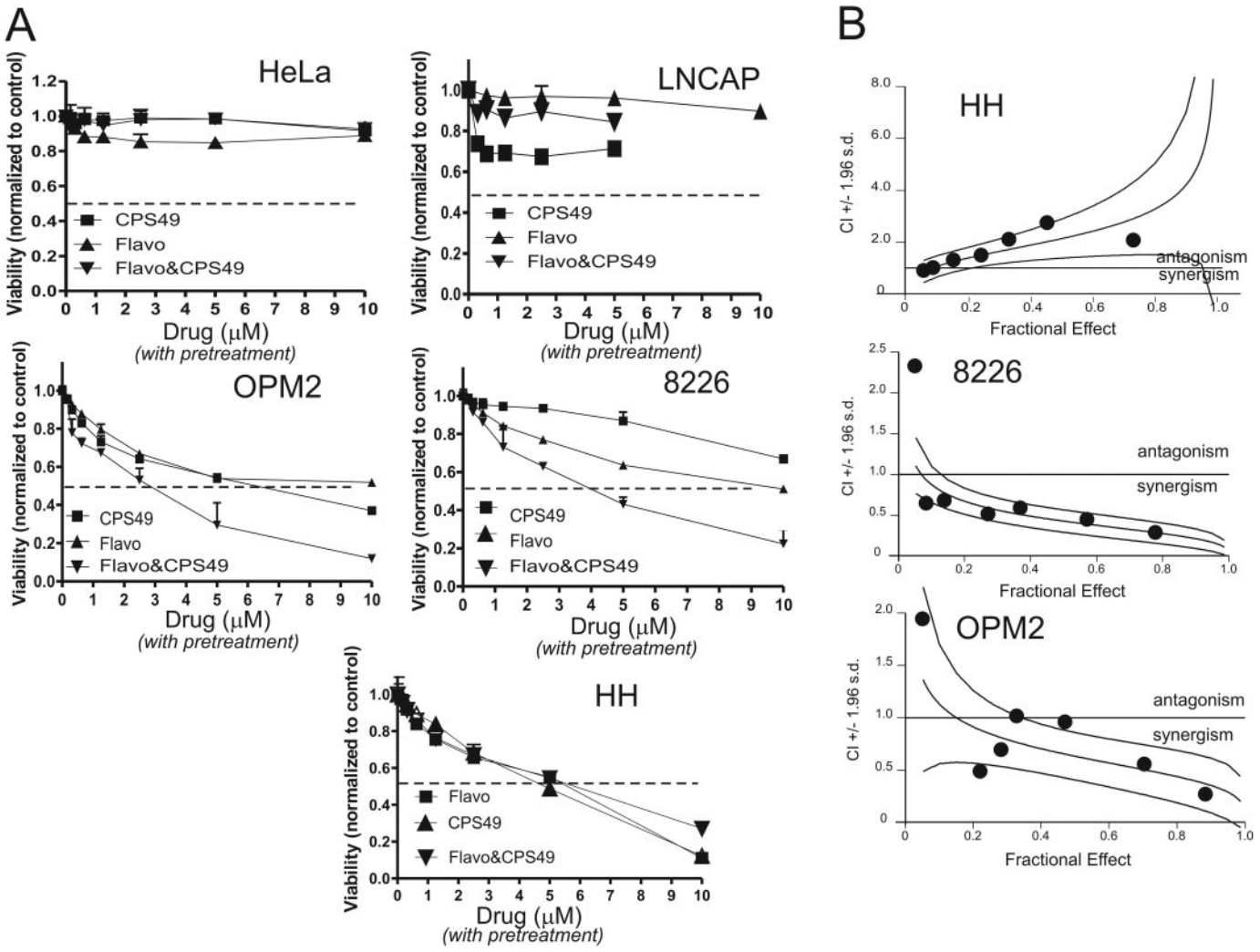

Fig. 5. The combinatorial synergy by CPS49 and flavopiridol after low-dose flavopiridol pretreatment is highly cell-type specific. A, HeLa, LNCaP, OPM2, 8226, and HH cell lines were incubated with increasing concentrations (0–10 μM) of CPS49 alone, flavopiridol alone, or CPS49 plus flavopiridol at a fixed ratio of 1:1. Cell viability was determined after 16-h incubation time with the drugs. B, CI values were determined for HH, OPM2, and 8226 and plotted against fractional effect to construct isobolograms. CI value < 1.0 indicates synergism, CI $= 1.0$ indicates an additive effect, and CI > 1.0 indicates antagonism. No isobologram for HeLa or LNCaP could be derived.

TABLE 3
Differential cell specificity of CPS49 and flavopiridol synergism following flavopiridol pretreatment

Cytotoxicity (MTT)											
8226				HH				OPM2			
CPS49	Flavo	Fa	CI	CPS49	Flavo	Fa	CI	CPS49	Flavo	Fa	CI
μM	μM			μM	μM			μM	μM		
0.15625	0.15625	0.0181	2.322	0.15625	0.15625	0.047	1.12	0.15625	0.15625	0.050	1.942
0.3125	0.3125	0.0864	0.65	0.3125	0.3125	0.085	1.33	0.3125	0.3125	0.220	0.488
0.625	0.625	0.1394	0.682	0.625	0.625	0.143	1.63	0.625	0.625	0.277	0.671
1.25	1.25	0.2697	0.508	1.25	1.25	0.237	1.95	1.25	1.25	0.325	1.012
2.5	2.5	0.3695	0.585	2.5	2.5	0.331	2.67	2.5	2.5	0.469	0.951
5	5	0.5695	0.443	5	5	0.455	3.47	5	5	0.704	0.559
10	10	0.7762	0.281	10	10	0.731	2.66	10	10	0.882	0.272

Fa, fraction affected by the dose; CI, combination index that defines additive effect or synergism or antagonism.

ment are likely to play a significant role. In this regard, it will be critical to determine the most effective pretreatment doses.

Because of the pleiotropic effects of both CPS49 and flavopiridol, there are some actions that are antagonistic. Because flavopiridol induces both G_1 and G_2 arrest, and cells are more sensitive to redox-reactive thalidomides in S-phase, it is not surprising that the cytotoxicity profile of the combination shows some antagonism. This antagonism is relieved by low-dose flavopiridol pretreatment, most likely because of the increased synergy for targeting mitochondrial function. This is also consistent with observations that flavopiridol can induce mitochondrial dysfunction as an early primary event independent of caspase activation (Litz et al., 2003). Why CPS49 seems to antagonize the ability of flavopiridol to stabilize E2F-1 activity is unclear, but the stress response induced by CPS49-mediated elevation of ROS could provide a signal that increases the phosphorylation of E2F-1 independent of Cdks. Alternatively, the drop in intracellular ATP levels associated with mitochondria-mediated necrotic cell death may also contribute to the antagonism against caspase-induced cell death, because apoptosomes require

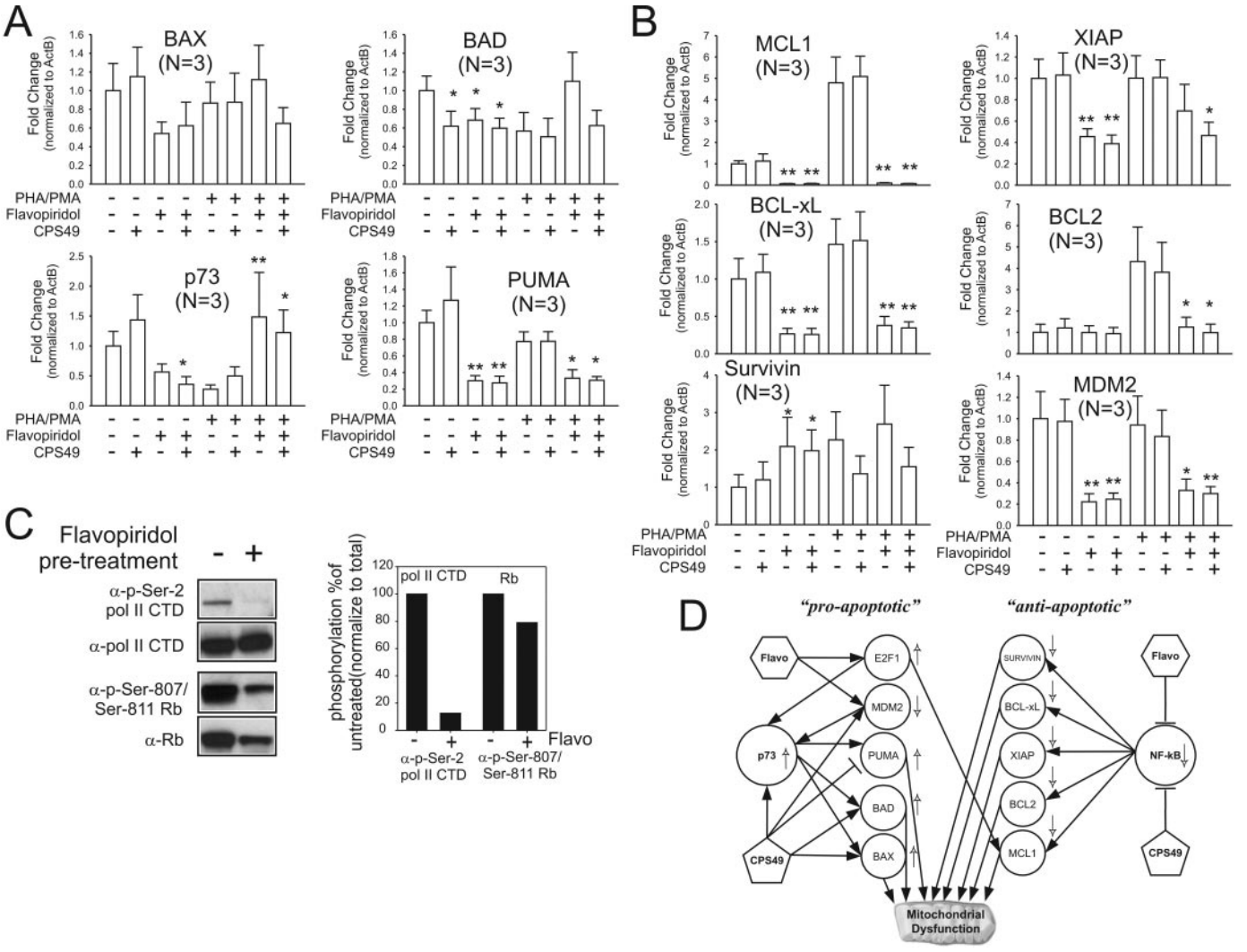

Fig. 6. Flavopiridol down-regulates genes important for mitochondrial stability and survival, but CPS49 shows lower efficacy in 8226 myeloma cells. A, 8226 myeloma cells were stimulated with 1 μg/ml PHA and 50 ng/ml PMA in the presence or absence of 10 μM CPS49 and/or flavopiridol for 3 h. Total cellular RNA was then isolated from the cell lysates, and cDNA was synthesized. mRNA levels of *BAX*, *BAD*, *p73*, and *PUMA* gene expression were analyzed by qRT-PCR. B, mRNA levels of *MCL1*, *XIAP*, *BCL-2*, *BCL-XL*, *Survivin*, and *MDM2* gene expression were assessed by qRT-PCR analysis in the 8226 cells treated with the drugs, as outlined above. The data presented are the means of three separate determinations after being normalized to those of the housekeeping gene β-actin. *, $P < 0.05$; **, $P < 0.01$ versus the untreated controls. C, Jurkat cells (10^7) were treated with and without 8-h pretreatment with 0.2 μM flavopiridol. Whole-cell lysates were prepared and analyzed by immunoblot for total and serine 2 C-terminal domain phosphorylated pol II and for total and serine 807/811 phosphorylated Rb. Shown at the right is a densitometer scan showing relative amount of serine 2 phosphorylated pol II compared with serine 808/811 phosphorylated Rb normalized to the total levels of each, respectively. D, This schematic diagram shows that CPS49 and flavopiridol increase *p73* directly or indirectly through sustaining the transcription factor E2F-1 and down-regulating *MDM2*. *p73* mediates mitochondrial dysfunction via either transcription of the proapoptotic genes *PUMA*, *BAD*, and *BAX* or mitochondrial localization of these proteins. On the other hand, CPS49 and flavopiridol induce cell death by inhibiting NF-κB and down-regulating NF-κB targeting antiapoptotic genes, such as *Survivin*, *XIAP*, *Bcl-2*, *Bcl-XL*, and *MCL1*. Because both CPS49 and flavopiridol cause mitochondrial damage through closely related but distinct mechanisms, they may act collaboratively or synergistically to promote apoptotic death of leukemia cells through p73 and NF-κB, and their downstream molecular events. Such a mechanism may serve to integrate the roles of p73 and NF-κB in culmination in mitochondrial damage and cell death, which may underlie the mechanism of CPS49 and flavopiridol-mediated mitochondrial dysfunction and cell killing in transformed leukemic cells.

ATP for function (Hu et al., 1999; Scholz et al., 2005). Finally the lack of synergy of the transcriptional targeting of both proapoptotic and antiapoptotic pathways in Jurkat suggest that the associated transcriptional pathways may be saturated by the compounds or there may be other undefined mechanisms where flavopiridol and CPS49 may act at different nodes within the transcription programs. The higher resistance of myeloma cells to CPS49 may also explain the similar lack of synergy in 8226.

As illustrated in Fig. 6D, CPS49 and flavopiridol can act in concert to enforce a transcriptional program that leads to cell-specific reciprocal up-regulation of proapoptotic effectors and down-regulation of antiapoptotic effectors. The ability of CPS49 to up-regulate *BAX*, *BAD*, and *p73* was unexpected, and the mechanism underlying this form of transcriptional target will require further investigation, however, because they are known p53 targets, the induction of *BAX*, *BAD* is most likely to be the result of p73 activation (Jurkat cells are p53-negative). Likewise, the down-regulation of *MDM2* by CPS49 occurs through a yet-to-be-defined mechanism in both Jurkat and myeloma; however, this could contribute to increased p53 and p73 transcriptional activity because MDM2 inhibits p73 function in the absence of degradation (Hu et al., 1999; Wang et al., 2001; Scholz et al., 2005). Although this influence of CPS49 was not seen in myeloma, it is tantalizing to speculate that further studies that examine pretreatment with different levels of flavopiridol may reveal a similar profile of transcriptional targeting by CPS49 in myeloma. How p73 is up-regulated transcriptionally by CPS49 remains unclear because, unlike flavopiridol, CPS49 does not increase E2F-1 levels. It is noteworthy that both CPS49 and flavopiridol are potent repressors of NF-κB activation, and their action together cooperatively represses p65 and I-κB phosphorylation in both resting and mitogen-activated cells. The I-κB kinase complex is responsible for these phosphorylation events and is therefore the likely direct target of both flavopiridol and CPS49. However, the robust effects of their combination suggest that their mechanism of the I-κB kinase complex targeting may not be the same. NF-κB repression is probably the major mechanism for the repression of the antiapoptotic genes in Fig. 6B, because all of these genes are known NF-κB targets. It will be interesting to assess whether the efficacy of targeting of these pathways by CPS49 in myeloma may be influenced by differential low-dose pretreatment with flavopiridol.

The addition of an ROS scavenger such as NAC produces slight rescue of leukemic cell viability and slightly represses the activation of PUMA and p73 by flavopiridol. This observation suggests a contribution of ROS to proapoptotic activation of these genes, however; the precise mechanism underlying this ROS influence will require further investigation.

In summary, we have profiled the efficacy of the combined use of flavopiridol and the redox-reactive thalidomide CPS49 and find that their concerted actions show selective cell-type-specific cytotoxicity against leukemic cells. The potency of their reciprocal targeting of general proapoptotic and antiapoptotic cellular pathways suggests that strategies involving differential adjustment of the dose and sequential addition of flavopiridol and redox-reactive thalidomides may lead to therapeutic benefit against a variety of human blood-borne cancers.

References

Blagosklonny MV (2004) Flavopiridol, an inhibitor of transcription: implications, problems and solutions. *Cell Cycle* **3:**1537–1542.

Chao SH and Price DH (2001) Flavopiridol inactivates P-TEFb and blocks most RNA polymerase II transcription in vivo. *J Biol Chem* **276:**31793–31799.

Chou TC and Talalay P (1984) Quantitative analysis of dose-effect relationships: the combined effects of multiple drugs or enzyme inhibitors. *Adv Enzyme Regul* **22:** 27–55.

Craig RW (2002) MCL1 provides a window on the role of the BCL2 family in cell proliferation, differentiation and tumorigenesis. *Leukemia* **16:**444–454.

Dai Y and Grant S (2003) Cyclin-dependent kinase inhibitors. *Curr Opin Pharmacol* **3:**362–370.

Decker RH, Dai Y, and Grant S (2001) The cyclin-dependent kinase inhibitor flavopiridol induces apoptosis in human leukemia cells (U937) through the mitochondrial rather than the receptor-mediated pathway. *Cell Death Differ* **8:**715–724.

Fiers W, Beyaert R, Declercq W, and Vandenabeele P (1999) More than one way to die: apoptosis, necrosis and reactive oxygen damage. *Oncogene* **18:**7719–7730.

Galluzzi L, Larochette N, Zamzami N, and Kroemer G (2006) Mitochondria as therapeutic targets for cancer chemotherapy. *Oncogene* **25:**4812–4830.

Ge Y, Montano I, Rustici G, Freebern WJ, Haggerty CM, Cui W, Ponciano-Jackson D, Chandramouli GV, Gardner ER, Figg WD, et al. (2006) Selective leukemic-cell killing by a novel functional class of thalidomide analogs. *Blood* **108:**4126–4135.

Gottlieb E and Thompson CB (2003) Targeting the mitochondria to enhance tumor suppression. *Methods Mol Biol* **223:**543–554.

Gottlieb E, Vander Heiden MG, and Thompson CB (2000) Bcl-x(L) prevents the initial decrease in mitochondrial membrane potential and subsequent reactive oxygen species production during tumor necrosis factor alpha-induced apoptosis. *Mol Cell Biol* **20:**5680–5689.

Grant S and Dent P (2004) Gene profiling and the cyclin-dependent kinase inhibitor flavopiridol: what's in a name? *Mol Cancer Ther* **3:**873–875.

Grant S and Roberts JD (2003) The use of cyclin-dependent kinase inhibitors alone or in combination with established cytotoxic drugs in cancer chemotherapy. *Drug Resist Updat* **6:**15–26.

Hitchens MR and Robbins PD (2003) The role of the transcription factor DP in apoptosis. *Apoptosis* **8:**461–468.

Hlavatá L, Aguilaniu H, Pichová A, and Nyström T (2003) The oncogenic RAS2(val19) mutation locks respiration, independently of PKA, in a mode prone to generate ROS. *EMBO J* **22:**3337–3345.

Hu Y, Benedict MA, Ding L, and Núñez G (1999) Role of cytochrome c and DATP/ATP hydrolysis in Apaf-1-mediated caspase-9 activation and apoptosis. *EMBO J* **18:**3586–3595.

Irwin M, Marin MC, Phillips AC, Seelan RS, Smith DI, Liu W, Flores ER, Tsai KY, Jacks T, Vousden KH, et al. (2000) Role for the P53 homologue P73 in E2F-1-induced apoptosis. *Nature* **407:**645–648.

Jiang J, Matranga CB, Cai D, Latham VM Jr, Zhang X, Lowell AM, Martelli F, and Shapiro GI (2003) Flavopiridol-induced apoptosis during s phase requires E2F-1 and inhibition of cyclin A-dependent kinase activity. *Cancer Res* **63:**7410–7422.

Kumar S, Raje N, Hideshima T, Ishitsuka K, Roccaro A, Shiraishi N, Hamasaki M, Yasui H, Munshi NC, Richardson P, et al. (2005) Antimyeloma activity of two novel N-substituted and tetraflourinated thalidomide analogs. *Leukemia* **19:**1253–1261.

Lam LT, Pickeral OK, Peng AC, Rosenwald A, Hurt EM, Giltnane JM, Averett LM, Zhao H, Davis RE, Sathyamoorthy M, et al. (2001) Genomic-scale measurement of MRNA turnover and the mechanisms of action of the anticancer drug flavopiridol. *Genome Biol* **2:**RESEARCH0041.

Lin A and Karin M (2003) NF-kappab in cancer: a marked target. *Semin Cancer Biol* **13:**107–114.

Litz J, Carlson P, Warshamana-Greene GS, Grant S, and Krystal GW (2003) Flavopiridol potently induces small cell lung cancer apoptosis during s phase in a manner that involves early mitochondrial dysfunction. *Clin Cancer Res* **9:**4586–4594.

Loewe S (1953) The problem of synergism and antagonism of combined drugs. *Arzneimittelforsch* **3:**285–290.

Luo JL, Kamata H, and Karin M (2005) The anti-death machinery in IKK/NF-kappab signaling. *J Clin Immunol* **25:**541–550.

Newcomb EW (2004) Flavopiridol: pleiotropic biological effects enhance its anticancer activity. *Anticancer Drugs* **15:**411–419.

Ng SS, Gütschow M, Weiss M, Hauschildt S, Teubert U, Hecker TK, Luzzio FA, Kruger EA, Eger K, and Figg WD (2003) Antiangiogenic activity of N-substituted and tetrafluorinated thalidomide analogues. *Cancer Res* **63:**3189–3194.

Ng SS, MacPherson GR, Gütschow M, Eger K, and Figg WD (2004) Antitumor effects of thalidomide analogs in human prostate cancer xenografts implanted in immunodeficient mice. *Clin Cancer Res* **10:**4192–4197.

Pei XY, Dai Y, and Grant S (2004) The small-molecule Bcl-2 inhibitor HA14-1 interacts synergistically with flavopiridol to induce mitochondrial injury and apoptosis in human myeloma cells through a free radical-dependent and Jun NH2-terminal kinase-dependent mechanism. *Mol Cancer Ther* **3:**1513–1524.

Pelicano H, Carney D, and Huang P (2004) ROS stress in cancer cells and therapeutic implications. *Drug Resist Updat* **7:**97–110.

Rosato RR, Almenara JA, Kolla SS, Maggio SC, Coe S, Giménez MS, Dent P, and Grant S (2007) Mechanism and functional role of XIAP and Mcl-1 down-regulation in flavopiridol/vorinostat antileukemic interactions. *Mol Cancer Ther* **6:**692–702.

Scholz C, Wieder T, Stärck L, Essmann F, Schulze-Osthoff K, Dörken B, and Daniel PT (2005) Arsenic trioxide triggers a regulated form of caspase-independent necrotic cell death via the mitochondrial death pathway. *Oncogene* **24:**1904–1913.

Sedlacek HH (2001) Mechanisms of action of flavopiridol. *Crit Rev Oncol Hematol* **38:**139–170.

Senderowicz AM, Headlee D, Stinson SF, Lush RM, Kalil N, Villalba L, Hill K, Steinberg SM, Figg WD, Tompkins A, et al. (1998) Phase I trial of continuous infusion flavopiridol, a novel cyclin-dependent kinase inhibitor, in patients with refractory neoplasms. *J Clin Oncol* **16:**2986–2999.

Shapiro GI (2004) Pre-clinical and clinical development of the cyclin-dependent kinase inhibitor flavopiridol. *Clin Cancer Res* **10:**4270S–4275S.
Shapiro GI (2006) Cyclin-dependent kinase pathways as targets for cancer treatment. *J Clin Oncol* **24:**1770–1783.
Takada Y and Aggarwal BB (2004) Flavopiridol inhibits NF-κB activation induced by various carcinogens and inflammatory agents through inhibition of IκBα kinase and P65 phosphorylation: abrogation of cyclin d1, cyclooxygenase-2, and matrix metalloprotease-9. *J Biol Chem* **279:**4750–4759.
Tan AR, Headlee D, Messmann R, Sausville EA, Arbuck SG, Murgo AJ, Melillo G, Zhai S, Figg WD, Swain SM, et al. (2002) Phase I clinical and pharmacokinetic study of flavopiridol administered as a daily 1-hour infusion in patients with advanced neoplasms. *J Clin Oncol* **20:**4074–4082.
Trachootham D, Zhou Y, Zhang H, Demizu Y, Chen Z, Pelicano H, Chiao PJ, Achanta G, Arlinghaus RB, Liu J, et al. (2006) Selective killing of oncogenically transformed cells through a ROS-mediated mechanism by beta-phenylethyl isothiocyanate. *Cancer Cell* **10:**241–252.
Wang XQ, Ongkeko WM, Lau AW, Leung KM, and Poon RY (2001) A possible role of P73 on the modulation of P53 level through MDM2. *Cancer Res* **61:**1598–1603.
Warfel NA, Lepper ER, Zhang C, Figg WD, and Dennis PA (2006) Importance of the stress kinase P38alpha in mediating the direct cytotoxic effects of the thalidomide analogue, CPS49, in cancer cells and endothelial cells. *Clin Cancer Res* **12:**3502–3509.
Wittmann S, Bali P, Donapaty S, Nimmanapalli R, Guo F, Yamaguchi H, Huang M, Jove R, Wang HG, and Bhalla K (2003) Flavopiridol down-regulates antiapoptotic proteins and sensitizes human breast cancer cells to epothilone B-induced apoptosis. *Cancer Res* **63:**93–99.
Zamzami N, Larochette N, and Kroemer G (2005) Mitochondrial permeability transition in apoptosis and necrosis. *Cell Death Differ* **12 (Suppl 2):**1478–1480.

Address correspondence to: Kevin Gardner, Laboratory of Receptor Biology and Gene Expression, National Cancer Institute, Building 41, Rm 41/D305, Bethesda, MD 20892-5065. E-mail: gardnerk@mail.nih.gov